forests

MDPI

Article

Thermal Conductivity of Poplar Wood Veneer Impregnated with Graphene/Polyvinyl Alcohol

Shuang-Shuang Wu [1], Xin Tao [2] and Wei Xu [1,3,*]

[1] College of Furnishings and Industrial Design, Nanjing Forestry University, Nanjing 210037, China; wushuangshuang@njfu.edu.cn
[2] Research Institute of Wood Industry, Chinese Academy of Forestry, Beijing 100091, China; taushin1994@163.com
[3] Co-Innovation Center of Efficient Processing and Utilization of Forest Resources, Nanjing Forestry University, Nanjing 210037, China
* Correspondence: xuwei@njfu.edu.cn; Tel.: +86-025-8542-7469

Abstract: Intending to achieve more green and economical graphene impregnated modified fast-growing poplar wood veneer for heat conduction, this study proposes and investigates the feasibility of modified veneer with graphene/Polyvinyl alcohol (Gr/PVA) impregnation mixture to improve its thermal conductivity. The absorbance and viscosity of the Gr/PVA impregnation mixtures are observed to expound the Gr/PVA ratio effects on the mixtures. Simultaneously, the weight percent gain, chromatic aberration, and thermal conductivity of the modified veneers are measured to determine the impregnation effect and the optimal impregnation formula. Further, the chemical structure, crystallinity, and thermal stability of the optimal sample impregnated with Gr/PVA are tested. The results show that the thermal properties of the Gr/PVA impregnated modified veneer have not all been improved. Still, both the dispersibility of the impregnation mixtures and the impregnation effect is affected by the Gr/PVA ratio. The data shows that the optimal thermal conductivity of modified veneer, which is up to 0.22 $W \cdot m^{-1} \cdot K^{-1}$ and 2.4 times the untreated one, is dipped by the mixture of 10 wt.% PVA concentration and 2 wt.% MGEIN addition. According to the characterization tests, the crystallinity of the modified veneer reduces, but the thermal stability improves.

Keywords: thermal conductivity; graphene; polyvinyl alcohol; wood veneers

check for updates

Citation: Wu, S.-S.; Tao, X.; Xu, W. Thermal Conductivity of Poplar Wood Veneer Impregnated with Graphene/Polyvinyl Alcohol. *Forests* **2021**, *12*, 777. https://doi.org/10.3390/f12060777

Academic Editors: Lina Nunes, Dennis Jones and Bruno Esteves

Received: 14 May 2021
Accepted: 10 June 2021
Published: 12 June 2021

Publisher's Note: MDPI stays neutral with regard to jurisdictional claims in published maps and institutional affiliations.

Copyright: © 2021 by the authors. Licensee MDPI, Basel, Switzerland. This article is an open access article distributed under the terms and conditions of the Creative Commons Attribution (CC BY) license (https://creativecommons.org/licenses/by/4.0/).

1. Introduction

Wood is an essential resource for construction and flooring, and the industry of wooden heating floors has a broad market in recent years. However, wood is a poor thermal conductor, mostly having its thermal conductivity less than 0.12 $W \cdot m^{-1} \cdot K^{-1}$ [1]. It has been proved that wood geometry, grain direction, density, moisture content, and porosity affect the thermal performance of wood [2,3]. The heat energy in the floor is conducted laterally, and the thermal conductivity in the horizontal direction is lower than the longitudinal direction [4]; hence, the heat transfer rate from bottom heating pipe units to the top flooring surface is low when the wood is used as a heated-flooring system during winter when heat is needed. Compared with solid wood, wood composites have better thermal conductivity; therefore, they are more suitable for heating floors. The wood composites commonly used for flooring include plywood, particleboard, high-density fiberboard, and thick veneers [5], whose thermal conductivities range from 0.12 to 0.17 $W \cdot m^{-1} \cdot K^{-1}$ [6]. Seo et al. [7] found that it was effective to increase the thermal conductivity of the wood flooring by using exfoliated graphite nanoplatelets (xGnP) or resin/xGnP composites as adhesive. Chen et al. [8] studied the thermal properties of four engineered wood floors with the same structure but different decorative veneers, revealing that the higher the density, the better the thermal conductivity. In short, there were numerous studies on heat transfer with the

condition of different floor heating structures [9,10]. However, limited studies have directly modified the thermal conductivity of wood used as a heated-flooring system [11].

Nanomaterials have excellent physical, mechanical, thermal, and magnetic properties [12,13]. Researchers have been using nanomaterials and nanotechnology to modify the wood to obtain wood-based nanocomposites with excellent properties for applications like preservation, weather resistance [14,15], flame retardance. Kong et al. [16] indicated that the photo-stability, flame retardance, and water-repelling properties of the wood surface could be improved through attaching zinc oxide (ZnO) nanorod arrays. Fan et al. [17] used the organic nano-montmorillonite (nano-OMMT) to enhance the thermal performance of wood fiber/HDPE composite and found that the thermal stability increased significantly as the nano-OMMT increased. In short, nanomaterials can help in improving the shortcomings of the thermal performance of the wood.

Graphene has been popular among scientific and engineering communities in recent years. Superior properties [18], like sizeable specific surface area and excellent crystallographic quality, making graphene-based nanomaterials have higher thermal, electrical conductivity, and mechanical strength. Therefore, graphene-based nanomaterials are widely used in composites, paints, capacitors, and batteries. The thermal conductivity of graphene-based nanomaterials ranges from 4000 to 5000 $W \cdot m^{-1} \cdot K^{-1}$ at room temperature, while single-layer graphene has its thermal conductivity up to 6000 $W \cdot m^{-1} \cdot K^{-1}$ [19]. Tang et al. [20] found that the thermal conductivity of epoxy resin could effectively increase up to 1900% when adding graphene materials into it and that graphene-modified epoxy resin had more excellent stability at high temperatures. Liem et al. [21] indicated a significant enhancement of thermal conductivity in epoxy resin nanocomposites added with single-layer graphene and boron nitride. Yang et al. [22] found that the synergistic effects of graphene and carbon nanotubes bettered the thermal performance of epoxy composites, which was related to the higher solubility and better compatibility of the multi-walled carbon nanotubes and the multi-graphene platelets (MWCNT/MGP). Hence, the value of graphene as efficient thermal functional filling materials has been proved.

Compared to the use of graphene in other polymer materials, there are fewer studies directly using graphene to improve the thermal properties of wood. Impregnation modification [23], a conventional method of modifying fast-growing wood, is a feasible way to fill wood with graphene. Tao et al. [24] prepared a thermal conductive floor using impregnation modification, taking phenol-formaldehyde resin as a carrying solution and graphene as a filler. The study revealed that the thermal conductivity of the modified wood had been improved, but the improvement effect was not ideal. Because when the graphene addition was low, the heat conduction of the graphene in the matrix resin was insufficient. While the amount was high, agglomeration occurred, which inhibited the conductivity of graphene itself.

Polyvinyl alcohol (PVA) is a degradable polymer with good water solubility, barrier properties, and film-forming properties so that it is widely used in the fields of papermaking, coatings, and biomedicine. It has been reported that PVA could enhance the adhesion and binding force in the preparation of highly water-stable and flexible conducting organic/inorganic composite materials with MWCNTs and carboxylic group functionalized graphene (GR-COOH) based on poly(3,4-ethylene dioxythiophene): poly (styrene-sulfonate) (PEDOT: PSS) dispersion [25]. In particular, Mehdi et al. [26] performed an experimental study on PVA-Gr to learn its colloidal stability in water and ethylene glycol. The results consistently confirmed that the readily miscible PVA functionalities made the Gr sheet form excellent colloidal stability.

Inspired by these aspects, a water-soluble-based PVA was used as the impregnating solution for mixing with graphene materials and impregnated into wood veneers. The absorbance and viscosity characterized the effects of the Gr/PVA ratio on the impregnation mixture. In contrast, influences of graphene material loading and PVA concentration on the thermal properties of wood veneers impregnated with Gr/PVA mixture were evaluated

through using the weight percent gain (*WPG*), the Fourier infrared spectroscopy (FT-IR), X-ray diffraction (XRD), and thermal gravity (TG).

2. Materials and Methods

2.1. Experimental Materials

The fast-growing poplar (Populus spp.) veneers sawed into the nominal dimensions of 100 mm long × 100 mm wide × 2 mm thick, and naturally seasoned to the moisture content of (13.8 ± 2)%, were provided by Dehua Tubao Decoration New Material Co., Ltd. (Deqing, China). The veneers were made of heartwood, and their average density was 0.38 kg/m^{-3}. All the veneers were polished to remove stains and burrs before use. The graphene material used in this experiment was multi-layered graphene-encapsulated iron nanoparticle (MGEIN) powders, provided by the Department of Sustainable Bioproducts, Mississippi State University, USA. The MGEIN diameter ranged from 400 to 600 nm. Polyvinyl alcohol (PVA) (Mw = 88,000, 87~89% hydrolyzed) was purchased from Nanjing Daguangming Chemical Reagent Co., Ltd. (Nanjing, China). Distilled water was homemade in the laboratory.

2.2. Experimental Design

A complete 3 × 4 factorial experiment with five replications per combination was conducted to evaluate factors that influence poplar wood veneers' thermal conductivity and stability. The two factors were PVA concentration in water (5, 10, 15 wt.%) and MGEIN powders loading (0, 1, 2, 3 wt.% of PVA solid content). Therefore, 60 veneers were evaluated in this study.

2.3. Procedure

The significant steps of impregnating a Gr/PVA mixture into fast-growing poplar wood veneers included the Gr/PVA mixture preparation, vacuum impregnation of the Gr/PVA mixture into poplar wood veneers, and the drying of impregnated veneers.

2.3.1. Impregnating Mixture Preparation

As shown in Figure 1, the polyvinyl alcohol solution was prepared in a water bath magnetically stirred for 2 h to avoid condensation. Then, the MGEIN powders were ball-grinded at 20 Hz vibration frequency for 30 min using a ball milling machine (Tehtnica Millmix 20, DOMEL), were added into the polyvinyl alcohol solution. The MGEIN powders loading was successively 1, 2, and 3 wt.% of the polyvinyl alcohol solid content. After magnetic stirring, the mixture was prepared. Furthermore, to improve the dispersion of MGEIN in the solution, the mixture was executed with ultrasonic processing for 20 min under a constant microwave irradiation power of 80 W. The Gr/PVA mixture was allowed to stand for at least 2 h before use.

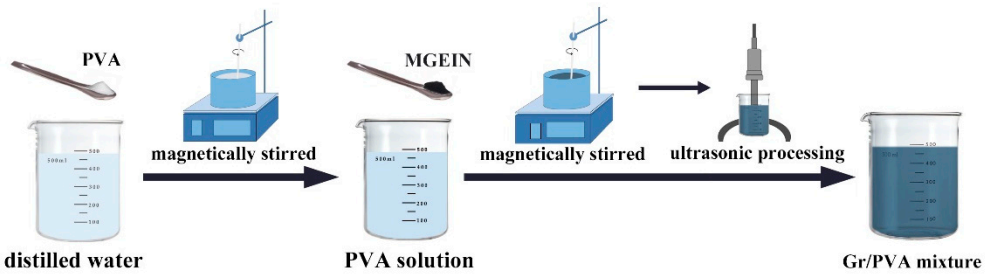

Figure 1. The preparation method of Gr/PVA impregnation mixture.

The impregnating mixture used for each veneer was 60 g, the specific formulations of the Gr/PVA impregnating mixture were shown in Table 1.

Table 1. The formulations of Gr/PVA impregnation mixture.

Number	PVA Concentration/wt.%	Ratio	MGEIN Powders Loading/wt.%(g)
GP-1	5	5 g PVA 100 mL Distilled Water	0(0)
GP-2			1(0.03)
GP-3			2(0.06)
GP-4			3(0.09)
GP-5	10	10 g PVA 100 mL Distilled Water	0(0)
GP-6			1(0.06)
GP-7			2(0.12)
GP-8			3(0.18)
GP-9	15	15 g PVA 100 mL Distilled Water	0(0)
GP-10			1(0.09)
GP-11			2(0.18)
GP-12			3(0.27)

2.3.2. Vacuum Impregnation

Five poplar veneers were randomly selected from the veneer supply for impregnating treatment with each of the 12 Gr/PVA mixtures. All veneers were oven-dried firstly at 80 °C in a drying oven (DHG-9643BS-III, CIMO) till reaching constant weights, followed by vacuum-impregnating each of the 12 Gr/PVA mixtures into these veneers in the vacuum drier (PC-3, Shanghai Sanshe Industry Co., Ltd.) under the treating condition of 60 min at 14 psi. Impregnated veneers were kept in the treating cylinder for 30 min [27] right after releasing the vacuum valve, followed by oven drying at 80 °C till constant weight was reached. The oven-dry weights of veneers before impregnation and after impregnation treatment were measured by an electronic scale (UTP-313, Hochoice).

2.4. Measurement and Characterization

2.4.1. Statistical Analysis

IBM SPSS Statistics performed a two-factor analysis of variance (ANOVA) general linear model (GLM) procedure to analyze the influence of different Gr/PVA ratios on the *WPG* and thermal conductivity. The partial Eta-squared was also calculated to measure the effect size of the PVA concentration and the MGEIN powders loading. All data analyses were performed at the 5% significance level.

2.4.2. Absorbance

The absorbance value is a reliable parameter that can reflect the dispersibility of the overall Gr/PVA impregnation mixtures. Each of the 12 impregnation mixtures diluted 2000 times was taken 5 mL into a quartz cuvette (1 mm thickness) for testing. The absorbance value at the 660 nm spectrum was measured by the UV-visible spectrophotometer (Lambda 950, PerkinElmer).

2.4.3. Viscosity

The viscosity value was measured by a digital display rotational viscometer (DVS, Brookfield). A total of 30 mL of Gr/PVA impregnation mixture was taken for testing 2 h after preparation, and the experiment temperature was controlled at (20 ± 2) °C.

2.4.4. Weight Percent Gain (*WPG*)

The weight percent gain (*WPG*) of treated veneers is an important indicator showing the Gr/PVA mixture content that impregnated into wood cells and vessels and left in the wood. The *WPG* value for each impregnated veneer was calculated by using the following Equation (1):

$$WPG = \frac{M_2 - M_1}{M_1} \times 100\% \quad (1)$$

where M_1 is the oven-dry weight (g) of veneers before impregnation treatment, and M_2 is the oven-dry weight of veneers after impregnation treatment.

2.4.5. Chromatic Aberration

The chromatic aberration is an intuitive parameter reflecting the impregnation condition of treated veneers. The treated veneers were tested at multiple points by a colorimeter (HP-2126, Zhuhai Tianchuang Instrument Co., Ltd., Zhuhai, China). The color values as L, a, and b were the average of multi-point measurements. The ΔE value for each impregnated veneer was calculated by using the following Equation (2):

$$\Delta E = \left[(\Delta L^2 + (\Delta a)^2 + (\Delta b)^2 \right]^{1/2} \quad (2)$$

where ΔE is the comprehensive evaluation index of color difference, ΔL is the brightness difference, Δa and Δb are the chroma difference.

2.4.6. Thermal Conductivity

In order to reduce the influence of moisture on the thermal conductivity, the samples were processed in the drying oven at a temperature of (103 ± 2) °C until the weight of the samples remained constant in two consecutive times so that they were considered absolutely dry. Besides, the samples were all polished with 200 grit sandpaper before testing. The thermal conductivity of impregnated veneers was measured by the YBF-4 thermal conductivity analyzer (Dahua, China) based on the steady-state plate method. The thermal conductivity λ ($W \cdot m^{-1} \cdot K^{-1}$) was calculated using the following Equation (3):

$$\lambda = mc \left. \frac{\Delta T}{\Delta t} \right|_{T=T_2} \cdot \frac{h}{T_1 - T_2} \cdot \frac{1}{\pi R^2} \quad (3)$$

where m is the weight of a copper heat sink (kg); c is the heat capacity of a copper heat sink ($J \cdot kg^{-1} \cdot K^{-1}$) with its value recorded as 385; $\left. \frac{\Delta T}{\Delta t} \right|_{T=T_2}$ is the heat dissipation rate of a copper heat sink at T_2 (mV/s); h is the thickness of tested veneers (m); T_1 is the temperature of the upper copper heat sink (K); T_2 is the temperature of the lower copper heat sink (K); $T_1 - T_2$ is the temperature difference between the upper and lower copper heat sinks (K); πR^2 is the area of the copper heat sink (m^2), 0.0133 m^2.

2.4.7. Fourier Infrared Spectroscopy (FT-IR)

Untreated poplar veneers (U–V), veneers impregnated with PVA (PVA–MW), veneers impregnated with Gr/PVA mixtures (GP–MW) were ground to 200 mesh powders using JI-ASOUND 800 °C grinder instrument (Hongtaiyang, China). The samples were mixed with potassium bromide at a mass ratio of 1:100 and ground into tablets for testing. FT-IR analysis of U–V, PVA–MW, and GP–MW powders was performed on a VERTEX 80 V instrument (Bruker, Germany). The resolution and wave ranges are 4 cm^{-1} and 4000~400 cm^{-1}.

2.4.8. X-ray Diffraction (XRD)

The crystallinity index of U–V, PVA–MW, and GP–MW powders was characterized using an Ultima IV X-ray diffractometer (Rigaku, Japan) in order to investigate the influence of the impregnation mixture on the structure of poplar veneer. The sample was ground to 200 mesh powders. Then, the dry sample powder was put into the slide groove until it flushed with the surface of the slide. The XRD scanning was performed ranging from 10° to 70°, and the target speed was 2 (°)·min^{-1}.

2.4.9. Thermal Gravity (TG)

The mass weight loss of U–V, PV–MW, and GP–MW powders was measured using a DTG-60 (Rigaku, Japan). A total weight of 10 mg of powders, ground to 200 mesh, was

used for each run. The testing atmosphere, heating rate, and temperature were N_2 gas, 20 °C/min, and 25~600 °C.

3. Results and Discussion

3.1. Gr/PVA Ratio Effects on Impregnation Mixtures

3.1.1. Absorbance

Figure 2 reveals the changes in absorbance of Gr/PVA impregnation mixtures with different Gr/PVA ratios. The absorbance of PVA solution with different PVA concentrations is almost unanimous. Since PVA gets evenly distributed when added to water, the solution is colorless and transparent, with no particles.

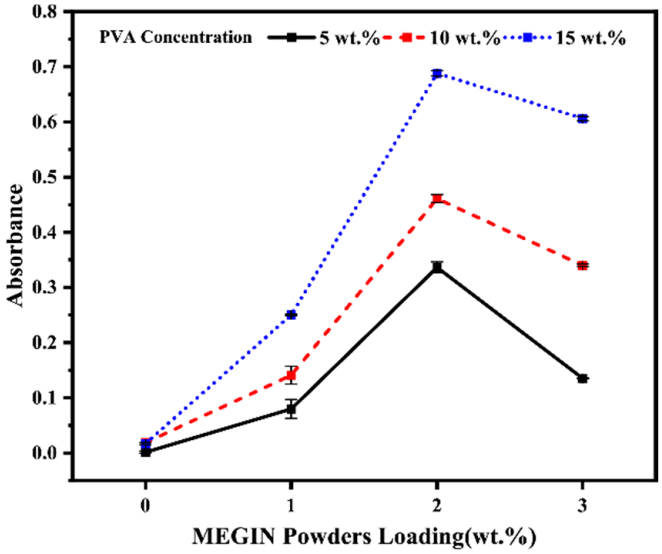

Figure 2. Absorbance of Gr/PVA impregnation mixture.

At the same PVA concentration, the effect of Gr/PVA ratio on the absorbance of Gr/PVA mixture has been investigated in MEGIN powders loading ranging from 0 to 3 wt.%. It has been observed that with an increase of MEGIN, the absorbance value increases stably at first. The rate becomes faster when MEGIN powders loading increases until attaining the maximum value at 2 wt.%. Afterwards, the absorbance value decreases with a further increase in MEGIN concentration. Due to the addition of MGEIN, the color of the impregnation mixture continues deepening. Therefore, the absorbance value increases constantly. However, it is difficult for PVA to suppress the Van der Waals force between many graphene sheets when the MEGIN concentration becomes higher. As a consequence, the graphene agglomerates, which result in the decrease of the absorbance value.

At the same MGEIN addition, the absorbance values of all the impregnation mixtures increased together with the increase of PVA. The optimum value was obtained for 2 wt.% PVA concentration. Compared with pure PVA solution, the absorbance values of 2 wt.% MGEIN addition in 5, 10, and 15 wt.% PVA solution increase by 20, 28, and 42 times, respectively, indicating that MGEIN disperses better in the solution with a higher PVA concentration.

According to the Rayleigh formula, the absorbance value is proportional to the concentration of particles in the suspension. The larger the absorbance value, the better the dispersion of the impregnation mixture. Therefore, under different MGEIN addition, the absorbance value at 5 wt.% PVA concentration is the lowest, indicating that MGEIN has the worst dispersibility at 5 wt.% PVA concentration. Similarly, MGEIN disperses better at 15 wt.% PVA concentration. In addition, the optimum ratio of Gr/PVA impregnation mixture, which has better dispersion, consists of 15 wt.% PVA and 2 wt.% MGEIN.

3.1.2. Viscosity

As shown in Figure 3, at the same MGEIN addition, the higher the concentration of the PVA solution, the greater the viscosity of the Gr/PVA impregnation mixtures. At the same time, the viscosity increases along with the increase of the MGEIN powders loading in the same PVA concentration. Specifically, a maximum rate, which is 167.1%, has been found at 10 wt.% PVA concentration with 3 wt.% MEGIN powders loading, while a minimum rate, which is 2.2%, has been found at 5 wt.% PVA concentration with 1 wt.% MEGIN powders loading. Furthermore, there is a significant difference in the viscosity of Gr/PVA impregnation mixtures with different PVA concentrations ($p = 0.001 < 0.05$). MGEIN has no noticeable thickening effect when dissolved in a low PVA concentration solution, while at high PVA concentration, it has an excellent thickening effect. These phenomena may be that the thickening effect of MGEIN partly depends on the type of dispersion medium and that MGEIN as a bridge forms interconnected networks between medium molecules, thus increasing viscosity when the medium has a high viscosity. This is consistent with previous research that graphene's sizeable specific surface area could form stronger nanoparticle-base fluid interactions [28].

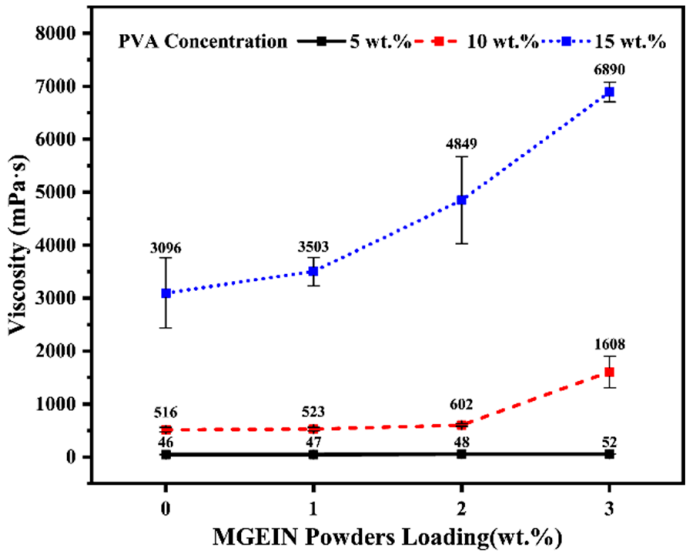

Figure 3. Viscosity of Gr/PVA impregnation mixtures.

3.2. Gr/PVA Ratio Effects on Veneer Characteristics

3.2.1. Gr/PVA Ratio Effects on Veneer *WPG*

Figure 4 shows the weight percent gains of Gr/PVA impregnated veneers. It can be seen from the picture that the *WPG* among different PVA concentrations at the same MGEIN addition is quite different. While at the same PVA concentration, the effect of MGEIN addition on the *WPG* is not obvious, especially at low concentrations, there is almost no change. At the same time, the *WPG* of the modified veneers shows a rapid increase first and then gradually changed, indicating that the ability of the wood to absorb the impregnation mixture has become saturated at this time and that the enhancement of MGEIN is limited. The ANOVA analysis and intersubjective effect test also attest that the PVA concentration ($p = 0.000 < 0.001$, $\eta_p^2 = 0.966$) has a particularly significant correlation with the *WPG*, while the MGEIN powders loading ($p = 0.028 < 0.05$, $\eta_p^2 = 0.757$) has a significant effect on the *WPG*, which shows that the PVA concentration has a more obvious influence on the *WPG*. Under the experimental parameters, when the PVA concentration is 15%, and the MGEIN powders loading is 3%, the *WPG* of the modified poplar veneers is the largest, which is 33%.

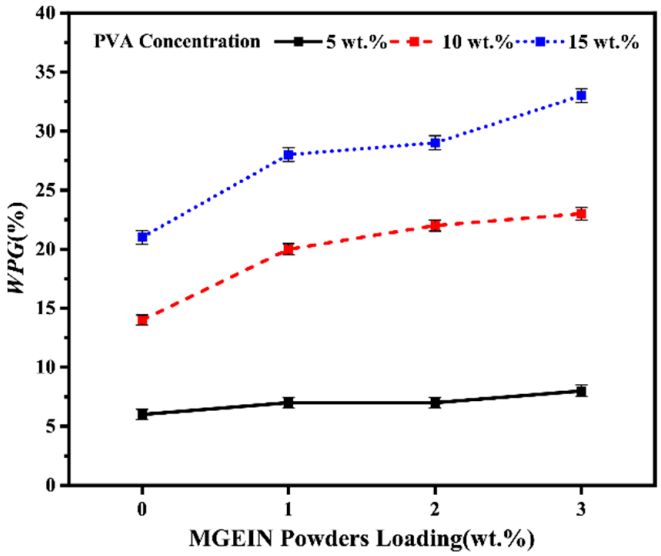

Figure 4. Weight percent gain of Gr/PVA impregnated modified veneers.

3.2.2. Gr/PVA Ratio Effects on Veneer Chromatic Aberration

Figure 5 visually shows the change of the veneers after dipping by Gr/PVA mixtures. It can be seen that the colors of the veneers (GP-1, GP-5, GP-9) immersed in PVA solution with different concentrations have no noticeable change and still appear pale white. In addition, the colors of those immersed in Gr/PVA appear light black. With the continuous addition of MGEIN, the color gradually becomes darker, but the distribution is uneven.

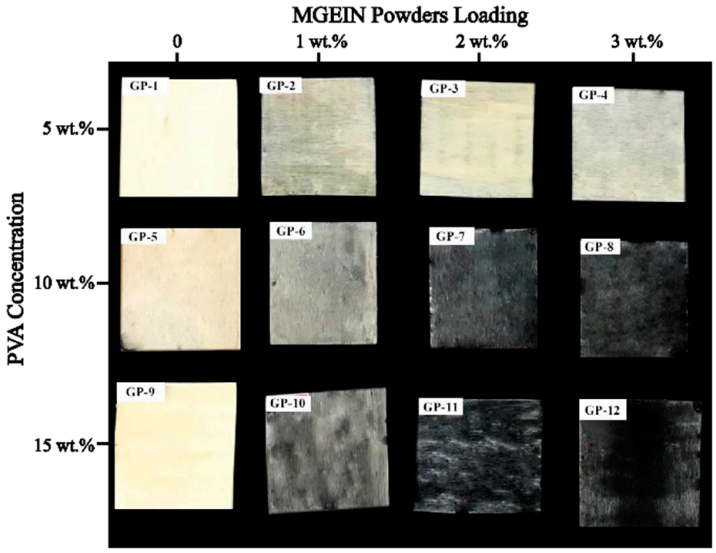

Figure 5. Colors of Gr/PVA impregnated modified veneers.

It is widely recognized that the larger the value of ΔE^*, the more significant difference between the treated veneer and untreated one will be. Thus, the chromatic aberration can intuitively characterize the impregnation effect. According to the CIE 1976 color difference formula, the change of value is shown in Figure 6. From the picture, we can see that the color difference values of the veneers, which were only dipped by the PVA solution with different concentrations, are similar and that those all distribute around 10.5, which is the same as the absorbance trend of Gr/PVA impregnation mixture. Therefore, the PVA concentration does not affect the color difference among the treated veneers, verifying that chromatic aberration can characterize the impregnation effect. It also reveals that the color difference value of Gr/PVA impregnated modified veneers has different increasing

trends at different PVA concentrations and the continuous addition of MGEIN. The value change is not evident at 5 wt.% PVA concentration, while it has a rapid increase at 10 wt.%, 15 wt.% PVA concentration. Moreover, it shows that the chromatic aberration values of the four treated veneers (GP-7, GP-8, GP-11, GP-12), which were dipped by higher PVA concentration (10 wt.%, 15 wt.%) and higher MGEIN powders loading (2 wt.%, 3 wt.%), tend to be close, ranging from 65 to 80. This fact indicates that the impregnation effect of treated veneers is roughly the same at higher PVA and MGEIN powders loading.

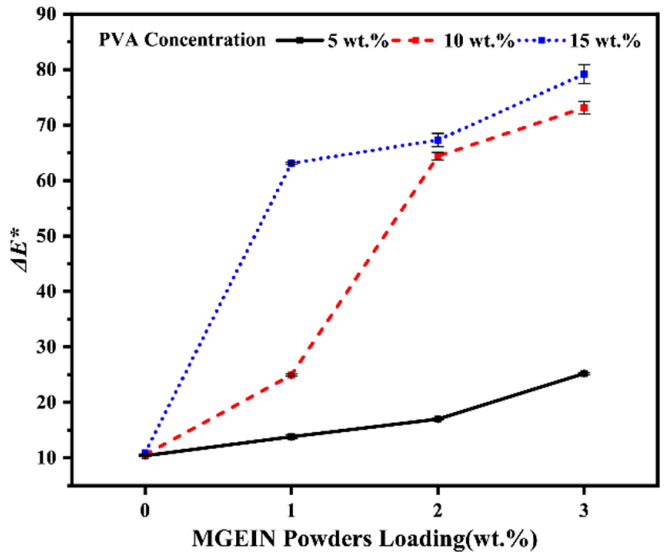

Figure 6. Chromatic aberration of Gr/PVA impregnated modified veneers.

3.2.3. Gr/PVA Ratio Effects on Veneer Thermal Conductivity

The changes of average density and thermal conductivity are shown in Figure 7. The result shows that at the same PVA concentration, the thermal conductivity of the treated veneer increases with the continuous increase of MGEIN until it reaches the best thermal conductivity at 2 wt.% MGEIN addition and then begins to decrease. The rule is also consistent with that of the absorbance of the Gr/PVA impregnation mixture, which illustrates that at the same PVA concentration, the better the dispersibility the Gr/PVA impregnation mixture, the higher the thermal conductivity of the modified veneer impregnated with it. In addition, we can see that at the same PVA concentration, the average density slowly increases with the MGEIN content, when at the same MEGIN addition, the higher the PVA concentration, the greater the average density increases. When the MGEIN powders loading is 0, 1 wt.%, 2 wt.%, the thermal conductivity of the modified veneer conforms to the general law in previous studies; that is, the thermal conductivity often tends to increase as the average density increase. However, when the MGEIN powders loading is 3 wt.%, the thermal conductivity dropped significantly. It may be explained that when the MGEIN powders loading is 3 wt.%, the dispersibility of the impregnation mixture is low, and the viscosity increases, causing the graphene to deposit on the surface without filling the cavities, the heat conduction path fails to appear. Therefore, an impregnation mixture with reduced dispersibility appears that even if its average density has increased, the thermal conductivity has shown a downward trend. Similarly, a previous study also revealed that as the content of PVA increased, the proportion of the heat transfer path through graphite decreased, leading to a decrease in the material's thermal conductivity [29]. At the same time, the ANOVA analysis and intersubjective effect test shows both the PVA concentration ($p = 0.02 < 0.05$, $\eta_p^2 = 0.630$) and the MGEIN powders loading ($p = 0.003 < 0.05$, $\eta_p^2 = 0.883$) have a significant effect on the thermal conductivity, but MGEIN powders loading plays a more critical role. This is consistent with the previous analysis.

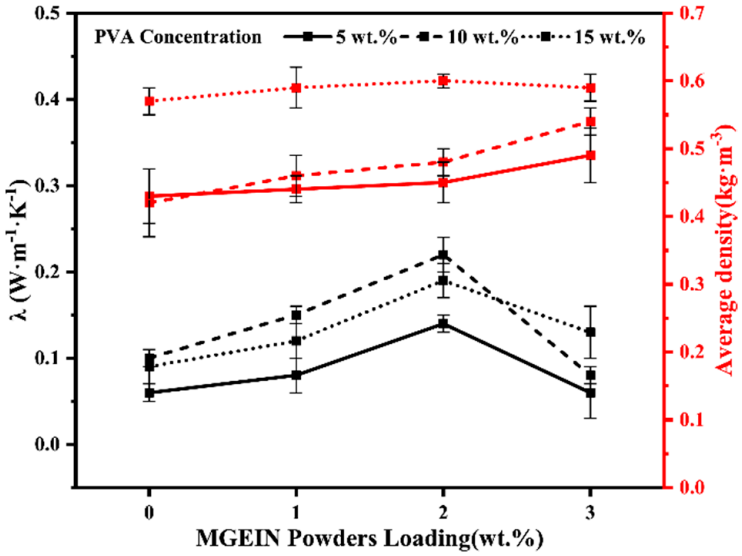

Figure 7. Thermal conductivity of Gr/PVA impregnated modified veneers.

The data in Table 2, in good agreement with these literature date for similar wood types [30], shows that the thermal conductivity of the Gr/PVA impregnated modified veneer has not all been improved compared with the untreated veneer (the control sample, 0.09 $W \cdot m^{-1} \cdot K^{-1}$). At 5 wt.% PVA concentration, the thermal conductivity of the treated veneer shows a downward trend, except for GP-3. While at 10 wt.%, 15 wt.% PVA concentration, compared with the untreated veneer dipped by the same PVA concentration solution, the addition of MGEIN can improve the thermal conductivity of the veneer, except for GP-8. The thermal conductivity of foamed film has also been increased and immersed in the wood's pores, so the treated veneer's thermal conductivity has also been improved. The results are also consistent with the above analysis.

Table 2. Thermal conductivity of Gr/PVA impregnated modified veneers.

Number	Λ($W \cdot m^{-1} \cdot K^{-1}$)	λ Growth Rate/%	
		Compared with Untreated Veneer	Compared with Veneer Dipped by the Same PVA Concentration Solution without MGEIN
GP-1	0.06	−33	/
GP-2	0.08	−11	33
GP-3	0.14	56	133
GP-4	0.06	−33	0
GP-5	0.10	11	/
GP-6	0.15	67	50
GP-7	0.22	144	120
GP-8	0.08	−11	−20
GP-9	0.09	0	/
GP-10	0.12	33	33
GP-11	0.19	111	111
GP-12	0.13	44	44

In order to further study the characteristic of the Gr/PVA impregnated modified veneer, the treated veneer GP-7 with the highest thermal conductivity, dipped by the 10 wt.% PVA concentration and 2 wt.% MGEIN addition impregnation mixture, was selected and referred to as GP–MW. The thermal conductivity of the selection is 0.22 $W \cdot m^{-1} \cdot K^{-1}$, which is 2.4 times that of untreated veneer.

3.3. GP-MW Characterization Analysis

3.3.1. FT-IR Analysis

Figure 8 is the FT-IR diagram of the highest thermal conductivity sample (GP–MW) and the sample impregnated with 10 wt.% PVA (PVA–MW) as the comparison with untreated veneer (U–V). There is a C-H stretching vibration of CH-3, CH-2 near 2900 cm^{-1}, a C=O stretching vibration close to 1730 cm^{-1}, and a C-O stretching vibration of cellulose, hemicellulose near 1030 cm^{-1} [31]. With the addition of MGEIN, the peak transmittance of GP-MW at 1029 cm^{-1} decreased, which indicates that the Gr/PVA impregnation mixture caused a decrease in the hydroxyl groups on the cellulose and that hydrogen bond association occurred.

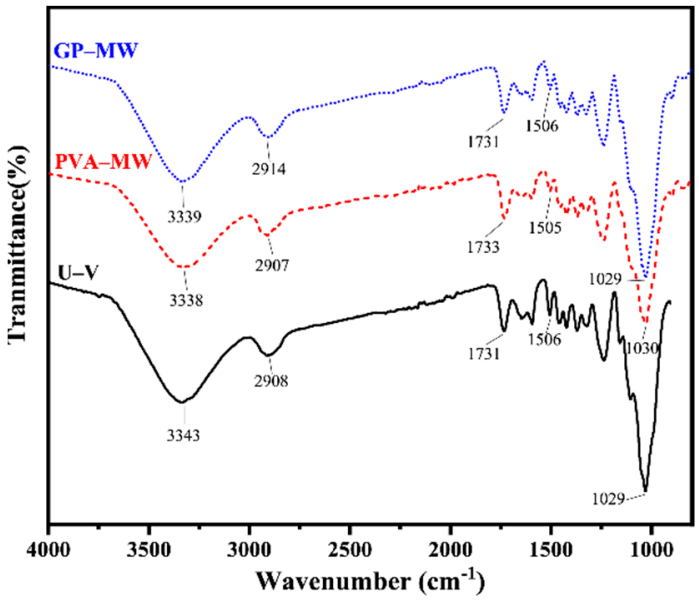

Figure 8. FT-IR spectra of untreated veneer, PVA, and Gr/PVA impregnated modified veneers.

It also can be seen that the three test samples all have an absorption peak near 3340 cm^{-1}. By comparison with U–V, there is a decrease in the peak transmittance of PVA–MW, which is moved to 3338 cm^{-1}. Moreover, the peak gradually weakened with the addition of MGEIN, revealing that the secondary valence bonds were broken, such as the intermolecular hydrogen bond, and that the intermolecular force weakened.

3.3.2. XRD Analysis

Figure 9 shows the XRD patterns of U–V, PVA–MW, GP–MW. The diffraction peak analysis of U–V shows apparent evolution around 17.0°, 22.2°, and 35.0°. The peaks represent the wood cellulose (100), (002), and (040) crystal faces [32]. It can be seen that compared with U–V, the GP–MV's diffraction intensity at 17.0° and 22.2° is weaker, and PVA–MW's at 35° almost appears, mainly due to lead to the decrease of the cellulose content, which is caused by the addition of PVA and MGEIN. Furthermore, calculated by the Turley method, the crystallinity of GP–MW is 0.50, which is close to PVA–MW, whose crystallinity is 0.49, illustrating that the structural properties of Gr/PVA impregnated veneer and pure PVA impregnated veneer are not much different. However, compared with the crystallinity of 0.62 of U–V, both PVA–MW and GP–MW decrease, indicating that MGEIN enters the modified veneer.

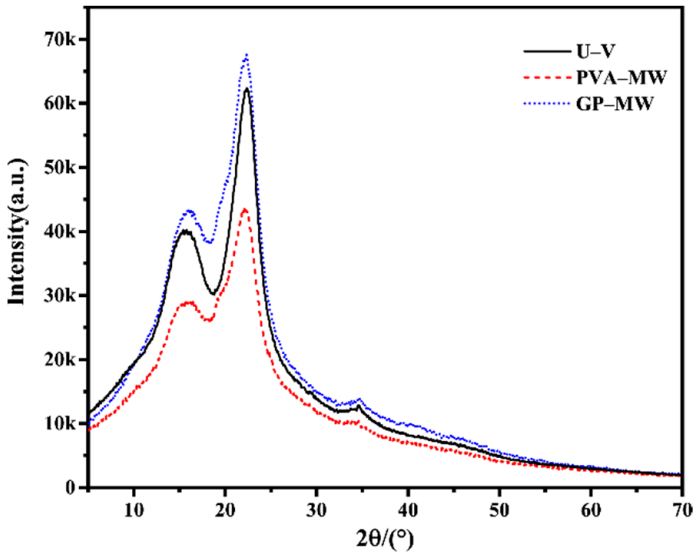

Figure 9. XRD of untreated veneer, PVA, and Gr/PVA impregnated modified veneers.

3.3.3. TG/DTG Analysis

The thermal stability of wood is directly related to the three natural polymers of cellulose, hemicellulose, and lignin. As temperature rises, the structure of the wood component will be gradually destroyed, the degradation will be carried out, and the internal components will be volatilized, resulting in the continuous reduction of the quality of the wood. The reaction between Gr/PVA mixture and wood can be analyzed [33].

Figure 10 is a graph of TG and DTG for the U–V, PVA–MW, and GP–MW. As shown in Figure 10a, the samples are divided into four thermal degradation stages. At the first stage, ranging from 30 to 100 °C, the mass loss rate is relatively low, where the mass rate of U–V, PVA–MW, and GP–MW is about 10, 7, and 8%, respectively. During this stage, the mass rate is mainly caused by volatile components in the veneer, such as the bound water. At the second stage ranging from 100 to 300 °C, the mass-loss rates of those are 23, 18, and 22%, respectively. That may be explained that the hemicellulose or part of the impregnation mixture begins to degrade in this temperature range. Due to the high-temperature oxidation of cellulose, the qualities of test pieces decrease, so the mass-loss rates, which are 33, 47, and 47%, respectively, are up to the largest at the third stage. The last stage is after 350 °C, where the quality loss is due to the decomposition of cellulose inside the wood. In addition, since the heat resistance of PVA is between wood and graphene, the heat resistance of GP–MW is also in a unified range after compounding.

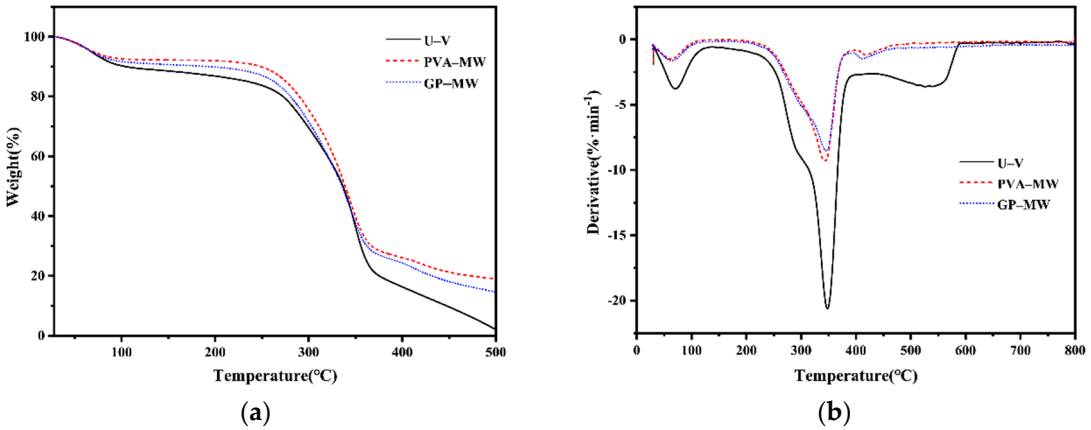

Figure 10. The TG and DTG for the untreated veneer, PVA and Gr/PVA impregnated modified veneers: (**a**) TG curves; (**b**) DTG curves.

From Figure 10b, it can be seen that compared with the DTG curve of U–V and PVA–MW, the mass loss rate of GP–MW is weaker with the increase of the decomposition temperature. That proves that the thermal stability of GP–MW has been improved, indicating that MGEIN has played an important role.

4. Conclusions

From the perspective of economy and environmental protection, a type of wood-based composite for heat conduction was prepared by being impregnated with Gr/PVA mixture to enhance the thermal conductivity of poplar wood veneer and promote its application in the heating floor. The major conclusions of this study are as follows:

- The *WPG* of the modified veneer increased with the PVA concentration and the content of the MGEIN powders. The PVA concentration plays a more critical role in *WPG*. Besides, the average density gradually increased with the *WPG*. The thermal conductivity of the modified veneer would increase as the average density increase. However, it would also be affected by other factors, especially at high PVA concentration and high MGEIN powders loading.
- At the same concentration of PVA, when the MGEIN powders loading is up to 2 wt.%, the dispersion effect of the Gr/PVA impregnation mixture is the best, and the thermal conductivity of the corresponding sample is also the greatest.
- The thermal conductivity of the modified veneer is the best at 10% PVA concentration with 2 wt.% MGEIN addition.
- Both FI-TR and XRD characterization results prove that the internal structure of the modified material has changed and that of MGEIN, which enters the amorphous region of the cellulose, reacts with the hydroxyl group in the amorphous region, resulting in a decrease in the crystallinity value.
- The TG analysis shows that the thermal stability of the Gr/PVA impregnated modified material has been improved. Therefore, the thermal properties of veneers could be improved by the Gr/PVA impregnation mixture, but the improvement effect is related to the dispersion and viscosity of the mixture to a certain extent.
- In addition, we can further study how to make graphene form a better heat channel inside the wood.

Author Contributions: Conceptualization, W.X.; methodology, X.T. and S.-S.W.; software, S.-S.W.; validation, W.X. and S.-S.W.; formal analysis, S.-S.W.; investigation, S.-S.W.; resources, W.X., X.T. and S.-S.W.; data curation, S.-S.W.; writing—original draft preparation, S.-S.W.; writing—review and editing, W.X. and S.-S.W. All authors have read and agreed to the published version of the manuscript.

Funding: This work was supported by A Project Funded by the National Key R&D Program of China (2017YFD0601104).

Data Availability Statement: The data presented in this study are available on request from the corresponding author.

Acknowledgments: The authors thank the college of Furnishings and Industrial Design of Nanjing Forestry University for supplying laboratories and equipment for this experiment. At the same time, we also thank the Department of Sustainable Bioproducts of Mississippi State University for providing the MGEIN. Finally, we are grateful to the reviewers and editors for their valuable time and suggestions for improving the quality of this paper.

Conflicts of Interest: The authors declare no conflict of interest.

References

1. Seo, J.; Jeon, J.; Lee, J.H.; Kim, S. Thermal performance analysis according to wood flooring structure for energy conservation in radiant floor heating systems. *Energy Build.* **2011**, *43*, 2039–2042. [CrossRef]
2. Vozár, L.; Labudová, G.; Babiak, M. Thermal diffusivity of selected wood species. *Wood Res.* **1999**, *44*, 1–8.
3. Krišťák, Ľ.; Igaz, R.; Ružiak, I. Applying the EDPS Method to the Research into Thermophysical Properties of Solid Wood of Coniferous Trees. *Adv. Mater. Sci. Eng.* **2019**, *2019*, 2303720. [CrossRef]
4. Kawasaki, T.; Kawai, S. Thermal Insulation Properties of Wood-Based Sandwich Panel for Use as Structural Walls and Floors. *J. Wood Sci.* **2006**, *52*, 75–83. [CrossRef]
5. Kim, S. Control of Formaldehyde and TVOC Emission from Wood-Based Flooring Composites at Various Manufacturing Processes by Surface Finishing. *J. Hazard. Mater.* **2010**, *176*, 14–19. [CrossRef] [PubMed]
6. Sonderegger, W.; Niemz, P. Thermal conductivity and Water Vapour Transmission Properties of Wood-Based Materials. *Eur. J. Wood Wood Prod.* **2009**, *67*, 313–321. [CrossRef]
7. Seo, J.; Cha, J.; Kim, S. Enhancement of the Thermal Conductivity of Adhesives for Wood Flooring Using xGnP. *Energy Build.* **2012**, *51*, 153–156. [CrossRef]
8. Chen, Q.Q.; Guo, X.L.; Ji, F.T.; Wang, J.; Cao, P.X. Effects of Decorative Veneer and Structure on the Thermal Conductivity of Engineered Wood Flooring. *Bioresources* **2015**, *10*, 2213–2222. [CrossRef]
9. Zhang, X.L.; Hao, X.L.; Hao, J.X.; Wang, Q.W. Heat Transfer and Mechanical Properties of Wood-Plastic Composites Filled with Flake Graphite. *Thermochim. Acta* **2018**, *664*, 26–31. [CrossRef]
10. Khorasanizadeh, H.; Sheikhzadeh, G.A.; Azemati, A.A.; Shirkavand Hadavand, B. Numerical Study of Air Flow and Heat Transfer in a Two-Dimensional Enclosure with Floor Heating. *Energy Build.* **2014**, *78*, 98–104. [CrossRef]
11. Lewis, C.S. Green Synthesis, Characterization, and Application of Metal-Based Nanomaterials. Ph.D. Thesis, Stony Brook University, New York, NY, USA, 2016.
12. Mcinerney, V. Computer Anxiety: Assessment and Treatment. Ph.D. Thesis, University of Tokyo Press, Tokyo, Japan, 1997.
13. De Filpo, G.; Palermo, A.M.; Rachiele, F.; Nicoletta, F.P. Preventing Fungal Growth in Wood by Titanium Dioxide Nanoparticles. *Int. Biodeterior. Biodegrad.* **2013**, *85*, 217–222. [CrossRef]
14. Yan, X.X.; Wang, L.; Qian, X.Y. Influence of the PVC of Glass Fiber Powder on the Properties of a Thermochromic Waterborne Coating for Chinese Fir Boards. *Coatings* **2020**, *10*, 588. [CrossRef]
15. Yan, X.X.; Zhao, W.T.; Qian, X.Y. Effect of Urea-Formaldehyde (UF) with Waterborne Emulsion Microcapsules on Properties of Waterborne Acrylic Coatings Based on Coating Process for American Lime. *Appl. Sci.* **2020**, *10*, 6341. [CrossRef]
16. Kong, L.Z.; Tu, K.K.; Guan, H.; Wang, X.Q. Growth of High-Density ZnO Nanorods on Wood with Enhanced Photostability, Flame Retardancy and Water Repellency. *Appl. Surf. Sci.* **2017**, *407*, 479–484. [CrossRef]
17. Fan, S.T.; Gao, X.; Zhu, D.J.; Guo, S.C.; Li, Z. Enhancement Mechanism of the Organic Nano-Montmorillonite and Its Effect on the Properties of Wood Fiber/HAPE Composite. *Ind. Crop. Prod.* **2021**, *169*, 113634. [CrossRef]
18. Balandin, A.A. Thermal Properties of Graphene and Nanostructured Carbon Materials. *Nat. Mater.* **2011**, *10*, 569–581. [CrossRef] [PubMed]
19. Yang, N.; Xu, X.F.; Zhang, G.; Li, B.W. Thermal Transport in Nanostructures. *AIP Adv.* **2012**, *2*, 041410. [CrossRef]
20. Tang, B.; Hu, G.X.; Gao, H.Y.; Hai, L.Y. Application of Graphene as Filler to Improve Thermal Transport Property of Epoxy Resin for Thermal Interface Materials. *Int. J. Heat Mass Transf.* **2015**, *85*, 420–429. [CrossRef]
21. Liem, H.; Choy, H.S. Superior Thermal Conductivity of Polymer Nanocomposites by Using Graphene and Boron Nitride as Fillers. *Solid State Commun.* **2013**, *163*, 41–45. [CrossRef]
22. Yang, S.Y.; Lin, W.N.; Huang, Y.L.; Tien, H.W.; Wang, J.Y.; Ma, C.C.M.; Li, S.M.; Wang, Y.S. Synergetic Effects of Graphene Platelets and Carbon Nanotubes on the Mechanical and Thermal Properties of Epoxy Composites. *Carbon* **2011**, *49*, 793–803. [CrossRef]
23. Hu, W.G.; ZHANG, J.L. Bolt-Bearing Yield Strength of Three-Layered Cross-Laminated Timber Treated with Phenol Formaldehyde Resin. *Forests* **2020**, *11*, 551. [CrossRef]
24. Tao, X.; Wu, Y.; Xu, W.; Zhan, X.X.; Zhang, J.L. Preparation and Characterization of Heating Floor Impregnated by Graphene /Phenol-Formaldehyde Resin. *J. For. Eng.* **2019**, *4*, 167–173.
25. Wang, Z.F.; Xu, J.K.; Yao, Y.Y.; Zhang, L.; Wen, Y.P.; Song, H.J.; Zhu, D.H. Facile Preparation of Highly Water-Stable and Flexible PEDOT:PSS Organic/inorganic Composite Materials and Their Application in Electrochemical Sensors. *Sens. Actuators B Chem.* **2014**, *196*, 357–369. [CrossRef]
26. Azizi, M.; Honarvar, B. Investigation of Thermophysical Properties of Nanofluids Containing Poly(vinyl alcohol)-Functionalized Graphene. *J. Therm. Anal. Calorim.* **2018**, *133*, 1259–1269. [CrossRef]
27. Vetter, L.D.; Depraetere, G.; Janssen, C.; Stevens, M.; Acker, J.V. Methodology to Assess Both the Efficacy and Ecotoxicology of Preservative-Treated and Modified Wood. *Ann. For. Sci.* **2008**, *65*, 504. [CrossRef]
28. Ranjbarzadeh, R.; Akhgar, A.; Musivand, S.; Afrand, M. Effects of Graphene Oxide-Silicon Oxide Hybrid Nanomaterials on Rheological Behavior of Water at Various Time Durations and Temperatures: Synthesis, Preparation and Stability. *Powder Technol.* **2018**, *335*, 375–387. [CrossRef]
29. Xie, W.; Zhou, Y.; Peng, S.W.; Kuang, J.C.; Zheng, Y.Y.; Yi, S.H.; Deng, Y.J. Thermal Analysis of Aphanitic Graphite/PVA Composites. *J. Funct. Mater.* **2015**, *47*, 3170–3174, 3180.

30. Özcan, C.; Korkmaz, M. Relationship between the Thermal Conductivity and Mechanical Properties of Uludağ Fir and Black Poplar. *Bioresources* **2018**, *4*, 8154–8184. [CrossRef]
31. Dan, R.; Teaca, C.A.; Bodirlau, R. Rosu, L. FTIR and Color Change of the Modified Wood as a Result of Artificial Light Irradiation. *J. Photochem. Photobiol. B* **2010**, *99*, 144–149.
32. Chen, H.Y.; Lang, Q.; Bi, Z.; Miao, X.W.; Li, Y.; Pu, J.W. Impregnation of Poplar Wood (Populus Euramericana) with Methylolurea and Sodium Silicate Sol and Induction of In-Situ Gel Polymerization by Heating. *Holzforschung* **2014**, *68*, 45–52. [CrossRef]
33. Müller, G.; Schöpper, C.; Vos, H.; Kharazipour, A.; Polle, A. FTIR-ATR Spectroscopic Analysis of Changes in Wood Properties during Particle and Fiberboard Production of Hard and Softwood Trees. *Bioresources* **2009**, *4*, 49–71.